ABT-888, an Orally Active Poly(ADP-Ribose) Polymerase Inhibitor that Potentiates DNA-Damaging Agents in Preclinical Tumor Models

Cherrie K. Donawho,[1] Yan Luo,[1] Yanping Luo,[1] Thomas D. Penning,[1] Joy L. Bauch,[1] Jennifer J. Bouska,[1] Velitchka D. Bontcheva-Diaz,[1] Bryan F. Cox,[1] Theodore L. DeWeese,[2] Larry E. Dillehay,[2] Debra C. Ferguson,[1] Nayereh S. Ghoreishi-Haack,[1] David R. Grimm,[1] Ran Guan,[1] Edward K. Han,[1] Rhonda R. Holley-Shanks,[1] Boris Hristov,[2] Kenneth B. Idler,[1] Ken Jarvis,[1] Eric F. Johnson,[1] Lawrence R. Kleinberg,[2] Vered Klinghofer,[1] Loren M. Lasko,[1] Xuesong Liu,[1] Kennan C. Marsh,[1] Thomas P. McGonigal,[1] Jonathan A. Meulbroek,[1] Amanda M. Olson,[1] Joann P. Palma,[1] Luis E. Rodriguez,[1] Yan Shi,[1] Jason A. Stavropoulos,[1] Alan C. Tsurutani,[1] Gui-Dong Zhu,[1] Saul H. Rosenberg,[1] Vincent L. Giranda,[1] and David J. Frost[1]

Abstract

Purpose: To evaluate the preclinical pharmacokinetics and antitumor efficacy of a novel orally bioavailable poly(ADP-ribose) polymerase (PARP) inhibitor, ABT-888.

Experimental Design: *In vitro* potency was determined in a PARP-1 and PARP-2 enzyme assay. *In vivo* efficacy was evaluated in syngeneic and xenograft models in combination with temozolomide, platinums, cyclophosphamide, and ionizing radiation.

Results: ABT-888 is a potent inhibitor of both PARP-1 and PARP-2 with K_is of 5.2 and 2.9 nmol/L, respectively. The compound has good oral bioavailability and crosses the blood-brain barrier. ABT-888 strongly potentiated temozolomide in the B16F10 s.c. murine melanoma model. PARP inhibition dramatically increased the efficacy of temozolomide at ABT-888 doses as low as 3.1 mg/kg/d and a maximal efficacy achieved at 25 mg/kg/d. In the 9L orthotopic rat glioma model, temozolomide alone exhibited minimal efficacy, whereas ABT-888, when combined with temozolomide, significantly slowed tumor progression. In the MX-1 breast xenograft model (BRCA1 deletion and BRCA2 mutation), ABT-888 potentiated cisplatin, carboplatin, and cyclophosphamide, causing regression of established tumors, whereas with comparable doses of cytotoxic agents alone, only modest tumor inhibition was exhibited. Finally, ABT-888 potentiated radiation (2 Gy/d $\times$ 10) in an HCT-116 colon carcinoma model. In each model, ABT-888 did not display single-agent activity.

Conclusions: ABT-888 is a potent inhibitor of PARP, has good oral bioavailability, can cross the blood-brain barrier, and potentiates temozolomide, platinums, cyclophosphamide, and radiation in syngeneic and xenograft tumor models. This broad spectrum of chemopotentiation and radiopotentiation makes this compound an attractive candidate for clinical evaluation.

Poly(ADP-ribose) polymerase (PARP)-1 is the founding member of a family of poly(ADP-ribosyl)ating proteins. All PARP family members are characterized by the ability to poly(ADP-ribosyl)ate protein substrates and all share a catalytic PARP homology domain (1). PARP-1 and the closely related PARP-2 are nuclear proteins and the only PARPs with DNA binding domains. These DNA binding domains localize PARP-1 and PARP-2 to the site of DNA damage serving as DNA damage sensors and signaling molecules for repair. The knockout of PARP-1 is sufficient to significantly impair DNA repair following damage via radiation (2) or cytotoxic (3) insult. The residual PARP-dependent repair activity ($\sim$10%) is due to PARP-2 (4, 5). These data imply that inhibition of only PARP-1 and PARP-2 will impair DNA repair following damage and that inhibition of other PARP family members is not required in the process. The functions of other PARP family members remain to be elucidated, but poly(ADP-ribosyl)ation has been implicated in many cellular processes, including differentiation, gene regulation, protein degradation, spindle maintenance, as well as replication and transcription (6).

Higher expression of PARP in cancer compared with normal cells has been linked to drug resistance and the overall ability of cancer cells to survive genotoxic stress (7, 8). Whereas PARP is ubiquitously expressed in almost all types of eukaryotic cells (9), PARP activity is increased in the nuclei of actively proliferating cells (1). Enhanced PARP-1 expression and/or

Authors' Affiliations: [1]Abbott Laboratories, Abbott Park, Illinois and [2]Department of Radiation Oncology and Molecular Radiation Sciences, The Johns Hopkins University School of Medicine, Baltimore, Maryland

Received 12/22/06; revised 2/11/07; accepted 2/13/07.

Grant support: Abbott Laboratories (Abbott Park, IL) to The Johns Hopkins University School of Medicine (T.L. DeWeese, L.E. Dillehay, B. Hristov, and L.E. Kleinberg).

The costs of publication of this article were defrayed in part by the payment of page charges. This article must therefore be hereby marked *advertisement* in accordance with 18 U.S.C. Section 1734 solely to indicate this fact.

Requests for reprints: David J. Frost, *In Vivo* Tumor Biology, Abbott Laboratories, R4N2 AP3, Abbott Park, IL 60064-6074. E-mail: david.frost@abbott.com.

©2007 American Association for Cancer Research.

doi:10.1158/1078-0432.CCR-06-3039

Downloaded from http://aacrjournals.org/clincancerres/article-pdf/13/9/2728/1974467/2728.pdf by guest on 28 February 2024

activity has been shown in several hematologic and solid tumors (7, 8, 10). This differential expression of PARP in normal versus tumor cells supports the observed selectivity of PARP inhibitors to affect proliferating tumor cells.

PARP activity is essential for the repair of ssDNA breaks through the base excision repair pathways (11, 12). Therefore, inhibition of PARP sensitizes tumor cells to cytotoxic agents that induce DNA damage that would normally be repaired through the base excision repair system (e.g., DNA glycosylase, AP endonuclease, XRCC1, etc.). The most notable agents in this group are alkylators (e.g., temozolomide and cyclophosphamide), topoisomerase I poisons (irinotecan and camptothecin), and certain types of intercalators (e.g., bleomycin). In fact, PARP inhibition has been shown to sensitize tumors to all of these agents (2, 13–16). Furthermore, PARP is involved in the repair of DNA from ionizing radiation, as numerous laboratories have shown that various PARP inhibitors sensitize cancer cells to radiation, both *in vitro* and *in vivo* (17, 18). PARP not only facilitates repair of ssDNA breaks but also binds to more lethal radiation-induced dsDNA breaks, apparently protecting the lesion and signaling repair (19). Consistent with the concept of PARP-1 as a radiosensitization target, PARP-1 knockout mice show enhanced sensitivity to γ-radiation (20, 21). Interestingly, some PARP inhibitors have been reported to show single-agent activity for tumors lacking BRCA1 or BRCA2 DNA double-stranded repair mechanisms (22, 23) and this is an active cancer research area (24).

As a result of chemopotentiation and radiopotentiation as well as potential for single-agent activity of PARP inhibitors, several PARP inhibitors have entered clinical trials for the treatment of cancer (24, 25). ABT-888 is a potent, orally bioavailable PARP inhibitor with good penetration into the brain. The compound is currently in the clinic for phase 0/Exploratory IND dose refinements and pharmacokinetic relationships (26). In this article, we describe the pharmacokinetic and antitumor activity (chemopotentiation and radiopotentiation) in preclinical animal models.

Materials and Methods

Compound. Enantiomerically pure ABT-888 was synthesized by Abbott Cancer Research and Process Chemistry. The synthesis and cell-based evaluation will be published elsewhere (27).

In vitro *PARP and SIRT assays.* PARP assays were conducted in a buffer containing 50 mmol/L Tris (pH 8.0), 1 mmol/L DTT, 1.5 μmol/L [^{3}H]NAD$^+$ (1.6 μCi/mmol), 200 nmol/L biotinylated histone H1, 200 nmol/L slDNA, and 1 nmol/L PARP-1 or 4 nmol/L PARP-2 enzyme. Reactions were terminated with 1.5 mmol/L benzamide, transferred to streptavidin Flash plates (Perkin-Elmer), and counted using a TopCount microplate scintillation counter.

Nicotinamide [2,5′,8-^{3}H]adenine dinucleotide and streptavidin SPA beads were purchased from Amersham Biosciences. Recombinant human PARP purified from *Escherichia coli* and 6-Biotin-17-NAD$^+$ were purchased from Trevigen. NAD$^+$, histone, aminobenzamide, 3-aminobenzamide, and calf thymus DNA (dcDNA) were from Sigma. Stem loop oligonucleotide (slDNA) CACAAGTGTTG*CATTCCT*C-TCTGAAGTTAAGACCTATGCAGAGAGGAATGCAACACTTGTG, containing MCAT sequence (italics), was obtained from Qiagen. The oligonucleotides were dissolved to 1 mmol/L in annealing buffer containing 10 mmol/L Tris-HCl (pH 7.5), 1 mmol/L EDTA, and 50 mmol/L NaCl, incubated for 5 min at 95°C, and followed by annealing at 45°C for 45 min. Histone H1 (95% electrophoretically pure) was purchased from Roche. Biotinylated histone H1 was prepared by treating the protein with Sulfo-NHS-LC-Biotin (Pierce). SIRT2 assays were conducted as described previously (28).

Pharmacokinetic studies. For oral pharmacokinetic studies, ABT-888 was separated from plasma and brain homogenate using liquid-liquid extraction with a mixture of ethyl acetate and hexane at alkaline pH. ABT-888 and the internal standard were separated from each other and coextracted contaminants on a 50 × 3 mm Keystone Betasil Cyano 5 μm C18 column with an acetonitrile: 0.1% trifluoroacetic acid mobile phase (40:60, by volume) at a flow rate of 0.3 mL/min. Analysis was done on a Sciex API3000 Biomolecular Mass Analyzer with a turbo-ionspray interface using Sciex MacQuan software (AME Bioscience). The analysis of plasma pharmacokinetics from osmotic minipump (OMP) studies was conducted using acidified methanol precipitated plasma. Samples were injected onto a Phenomenex Synergi 4μ Polar RP column and ABT-888 eluted with a mixture of acetonitrile and 0.1% acetic acid in water at a flow rate of 0.4 mL/min. Mass analysis was done with a ThermoFinnigan LCQ Duo using Xcalibur software (Thermo Electron Corp.).

Poly(ADP-ribose) polymer immunoblot. Tumors were excised and flash frozen in liquid nitrogen. Frozen tumors were quickly homogenized in PBS supplemented with 20 mmol/L EDTA on ice using a 70-μm cell strainer (BD Biosciences) to enrich for tumor cells. H&E analysis revealed 5% to 20% stromal interactions in the tumor. Single-cell suspensions were clarified of cell debris by a slow spin (20 × g, 5 min), then washed, pelleted, and lysed in cell extraction buffer (Invitrogen) supplemented with complete protease inhibitor (Roche Applied Science) for an hour at 4°C. Subsequently, lysates were pulse sonicated before clarification (300 × g at 4°C, 15 min). Protein concentration of lysates was assessed using the detergent-compatible protein assay per manufacturer's instructions (Bio-Rad). Samples were analyzed by immunoblotting using SuperSignal chemiluminescent system (Pierce). Rabbit polyclonal antibody for PAR was purchased from Trevigen (1:1,000) and β-tubulin rabbit polyclonal antibody was purchased from Cell Signaling Technology (1:1,000).

BRCA sequencing. All exons of *BRCA1* and *BRCA2* were sequenced as described previously (29).

Cell lines for* in vivo *studies. B16F10 syngeneic murine melanoma, 9L syngeneic rat glioma, and HCT-116 human colon carcinoma were obtained from the American Type Culture Collection (Manassas, VA) and cultured according to their recommendations. The DOHH-2 human B-cell lymphoma was obtained from the German Collection of Microorganisms and Cell Cultures. The lines were maintained at 37°C in a humidified atmosphere equilibrated with 5% CO_2, 95% air. The MX-1 human breast carcinoma was obtained from National Cancer Institute (Frederick, MD). MX-1 tumors for cisplatin experiments were propagated in *nude* mice by serial passage, whereas severe combined immunodeficient (*scid*) female mice were used for the carboplatin and cyclophosphamide experiments.

In vivo *chemopotentiation and irradiation studies.* All animal studies were conducted in accordance with the guidelines established by the internal Institutional Animal Care and Use Committees. The cisplatin potentiation study was conducted at the Cancer Therapy and Research Center, Institute for Drug Development (San Antonio, TX) and the radiation potentiation study was conducted at The Johns Hopkins University School of Medicine (Baltimore, MD). All other experiments were conducted at Abbott Laboratories (Abbott Park, IL). For B16F10 syngeneic studies, 6×10^4 cells were mixed with 50% Matrigel (BD Biosciences) and inoculated by s.c. injection into the flank of 6- to 8-week-old female C57BL/6 mice (20 g; Charles River Laboratories). Mice were injection-order allocated to treatment groups, and therapy was initiated on day 1 following inoculation. MX-1 tumors were established from an *in vivo* propagated line. For cisplatin efficacy studies, female *nude* mice (Harlan) were implanted s.c. by trocar with fragments (20-30 mm^3) of human tumors harvested from s.c. grown tumors in *nude* mice hosts. When the tumors were ~75 to 100 mm^3 in size, the animals were pair matched into treatment groups. For the

Downloaded from http://aacrjournals.org/clincancerres/article-pdf/13/9/2728/1974467/2728.pdf by guest on 28 February 2024

carboplatin and MX-1 cyclophosphamide studies, female *scid* mice (Charles River Laboratories) were inoculated with 200 μL of a 1:10 dilution of tumor brei in 45% Matrigel and 45% Spinner MEM (Life Technologies). For these established tumor studies, tumors were allowed to grow to the indicated size and then randomized to therapy groups. For DOHH-2 xenograft studies, 1×10^6 cells were mixed with 50% Matrigel and inoculated by s.c. injection into the flank of male *scid* mice (Charles River Laboratories). The tumors were allowed to grow to a predetermined size, then mice were randomized into therapy groups, and dosing was initiated. Tumor growth for experiments was analyzed by measurement with digital calipers and tumor volume was estimated from the formula $(L \times W^2) / 2$. Effects on tumor growth rate were assessed by determining %T/C [(mean tumor volume of treated group on day X / mean tumor volume of control group on day X) × 100] for a given treatment relative to monotherapy treatment. Effects on tumor growth delay were assessed by Kaplan-Meier analysis.

For the orthotopic glioma model, 12-week-old female Fischer 344 rats (160-170 g; Charles River Laboratories) were anesthetized with an i.p. injection of 70 mg/kg ketamine and 10 mg/kg xylazine. The rat head was immobilized using a stereotactic device. Following a small incision over the right hemisphere, a burr hole was prepared through the skull 2 mm anterior and 2 mm lateral to the bregma. Five microliters of cell suspension containing 5×10^5 tumor cells were injected 4 mm in depth into the rat brain via a 10-μL Hamilton syringe. The burr hole was bone wax sealed to reduce extracerebral leakage. The incision was closed with veterinary adhesive and rats were allowed to recover. Tumor growth was evaluated using T_1-weighted magnetic resonance imaging with a contrast enhancement by Magnevist (Berlex Laboratories) on days 8, 11, and 14 posttumor inoculation.

ABT-888 was delivered by either oral route or continuous infusion using s.c. placement of 14-day Alzet OMP model 2002 (Durect Corp.) in a vehicle containing 0.9% NaCl adjusted to pH 4.0. The OMP delivers at a rate of 12 μL daily and ABT-888 doses were calculated accordingly. Temozolomide (Schering-Plough), cisplatin (Bedford Laboratories), carboplatin (Bristol-Myers Squibb Co.), and cyclophosphamide (Bristol-Myers Squibb) were formulated according to the manufacturers' recommendations.

For radiation studies, five million human colon carcinoma HCT-116 cells were inoculated s.c. into the thighs of 6- to 7-week-old male *nude* mice and measured twice weekly at three perpendicular tumor dimensions. Tumor volume was calculated as (0.52) times the product of the three dimensions. When tumor volumes were between 0.20 and 0.30 cm^3, OMPs containing drug were implanted s.c. in the flank. Three days after the pump implantation, radiation treatments were begun. Radiation consisted of 2 Gy (at 5.9 Gy/min) delivered on 10 consecutive days to the tumor-bearing leg from a ^{137}Cs irradiator (Mark I, Shepherd and Associates), with the remainder of the body shielded from the source. Tumor response was determined from the number of days for each tumor to reach four times its volume at the start of the radiation treatments.

Statistical analysis. Differences between specified groups were analyzed using the Student's *t* test (two-tailed) for comparing two groups with $P < 0.05$ considered statistically significant. Kaplan-Meier method was used to determine median survival times (log-rank tests) for comparisons of ABT-888 combination plus cytotoxic agent versus cytotoxic alone (StatView software, SAS Institute, and GraphPad Prism, GraphPad Software, Inc.). In all tumor growth curves, mean tumor volumes indicate that all animals were present in the treatment group. Once a mouse is removed from the group, plotting was ceased.

Results

Activity of ABT-888. The chemical structure of 2-[(*R*)-2-methylpyrrolidin-2-yl]-1*H*-benzimidazole-4-carboxamide is shown in Fig. 1. ABT-888 is a potent PARP inhibitor, inhibiting PARP-1 and PARP-2 with K_is of 5.2 and 2.9 nmol/L, respectively. ABT-888 was also tested against SIRT2, an enzyme that also uses NAD^+ for catalysis, and found to be inactive (>5,000 nmol/L). The receptor profile of ABT-888 was determined in a panel of 74 receptor-binding assays at a concentration of 10 μmol/L (30). ABT-888 displaced control-specific binding at 50% or greater at the human H_1 (61%), the human 5-HT_{1A} (91%), and the human 5-HT_7 (84%) sites only. The IC_{50} values for these three receptors were 5.3, 1.5, and 1.2 μmol/L, respectively. These data indicate that ABT-888 exhibits a selective biochemical profile and that is unlikely to have adverse effects mediated by a wide range of receptors and ion channels at pharmacologically relevant plasma concentrations.

Pharmacokinetic studies. The pharmacokinetics of ABT-888 was evaluated in CD-1 mice, rats, dogs, and monkeys. (Table 1). ABT-888 is characterized by plasma clearance values between 0.6 to 4.1 L/h•kg, moderate volumes of distribution (V_{ss} = 2.0-3.1 L/kg), and terminal elimination half-lives of 1.2 to 2.7 h. The oral bioavailability from a solution formulation was 56% to 92%. Exposures were also obtained for both oral and OMP administration routes at multiple doses in C57BL/6, *nude*, and *scid* mice, the strains used in accessing preclinical efficacy. Exposures were similar across strains whether administration was oral or via OMP and were proportional with OMP (Table 1) and oral doses (data not shown).

ABT-888 potentiates temozolomide in a syngeneic melanoma model. Temozolomide is a newer generation of cytotoxic alkylating agent that is currently used to treat central nervous system malignancies and melanoma. The pharmacokinetic profile of temozolomide is similar between mice and humans, and this allows studies in mice at similar exposures to those achieved in humans. This is important because preclinical models best predict clinical outcomes when plasma drug concentrations of the cytotoxic agents are similar to those seen in humans (31). Consequently, a dose of 50 to 62.5 mg/kg/d temozolomide was used, and this dose closely mimics human exposure at the clinically relevant dose of 200 mg/m^2 (oral, q.d.×5) when measured by either area under the concentration curve (AUC) or C_{max}. At this dose range, no overt toxicity (e.g., excessive weight loss, ruffled coats, dehydration, etc.) was observed in mice.

The B16 model, which is relatively resistant to most chemotherapeutics, is moderately sensitive to temozolomide

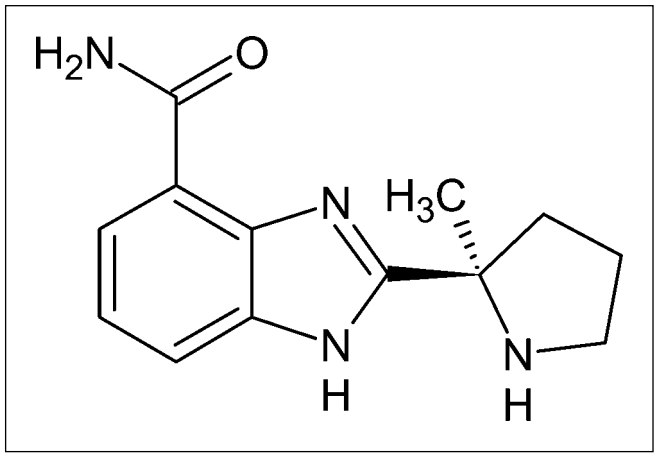

Fig. 1. Chemical structure of ABT-888 ($C_{13}H_{16}N_4O$, 244.29 g/mol).

Downloaded from http://aacrjournals.org/clincancerres/article-pdf/13/9/2728/1974467/2728.pdf by guest on 28 February 2024

Table 1. Pharmacokinetics of ABT-888 in mice, Sprague-Dawley rats, beagle dogs, and cynomolgus monkeys

i.v. Dose

Strain	Dose (mg/kg)	$t_{1/2}$ (h)	V_c (L/kg)	V_{ss} (L/kg)	V_β (L/kg)	AUC (μg•h/mL)	CL_p (L/h•kg)
Mouse CD-1	10	1.6	2.1	2.5	9.4	2.43	4.1
Rat	5	1.2	1.6	3.1	3.6	2.46	2.0
Dog	2.5	2.7	1.4	2.0	2.2	4.42	0.6
Monkey	2.5	1.9	2.0	2.8	3.1	2.36	1.1

Oral dose

Strain	Dose* (mg/kg)	C_{max} (μg/mL)	T_{max} (h)	$t_{1/2}$ (h)	$AUC_{0\text{-}12h}$ (μg•h/mL)	F (%)
Mouse CD-1	10	1.6	0.3	1.3	2.24	92
Rat	5	0.5	0.8	1.6	1.52	62
Dog	2.5	2.7	0.8	0.5	3.22	73
Monkey	2.5	2.5	0.3	2.3	1.33	56
Nude	12.5	0.8	0.7	1.0	1.30	
Scid	12.5	0.7	0.7	0.8	0.80	
C57BL/6	12.5	1.2	0.3	1.4	1.50	

OMP

Dose (mg/kg)	*Nude*		*Scid*		C57BL/6	
	C_{ss} (μg/mL)	$AUC_{0\text{-}24h}$ (μg•h/mL)	C_{ss} (μg/mL)	$AUC_{0\text{-}24h}$ (μg•h/mL)	C_{ss} (μg/mL)	$AUC_{0\text{-}24h}$ (μg•h/mL)
50	0.261	6.26	0.232	5.56	0.105	2.52
25	0.181	4.34	0.129	3.10	0.046	1.10
12.5	0.073	1.75	0.085	2.04		
5					0.022	0.53
3.125	0.023	0.55	0.017	0.41		

*In tumor models, the oral dose is administered b.i.d, so the total daily dose in milligrams per kilogram is doubled. Likewise, the $AUC_{0\text{-}12h}$ is multiplied by two to yield the total daily AUC.

and its sensitivity can be enhanced with PARP inhibitors (16, 32). ABT-888, administered orally, significantly potentiated the temozolomide efficacy in a dose-dependent manner (Fig. 2A). Maximum potentiation was seen at day 19 with % T/C values (versus temozolomide) of 10 ($P = 0.0003$), 16 ($P < 0.0001$), and 23 ($P < 0.0001$) for the 25, 12.5, and 3.1 mg/kg/d ABT-888 combination groups, respectively. The combinations were well tolerated with maximum body weight loss of 11% for the 25 mg/kg/d ABT-888 and temozolomide combination compared with 7% for temozolomide and 2% for ABT-888. The mice rapidly regained weight once the dosing period ended.

To establish the steady-state concentration necessary for *in vivo* activity, ABT-888 was administered as a continuous infusion in combination with 50 mg/kg/d temozolomide. ABT-888 at doses of 25 to 1 mg/kg/d all significantly potentiated the temozolomide monotherapy (Fig. 2B). Maximum potentiation was seen at day 17 with % T/C values (versus temozolomide) of 13 ($P < 0.0001$), 12 ($P < 0.0001$), 16 ($P < 0.0001$), 39 ($P = 0.0033$), and 63 (not significant) for the 25, 12.5, 5, 1, and 0.3 mg/kg/d ABT-888 combination groups, respectively. A higher dose of 50 mg/kg/d ABT-888 could not be evaluated with temozolomide because this combination resulted in skin toxicity at the OMP implantation site. The 25 and 12.5 mg/kg/d ABT-888 combination treatments were equivalent in activity, thereby defining the maximally efficacious dose as 12.5 mg/kg/d in this model. Maximum weight loss for the combination groups was 1% compared with a 5% gain for temozolomide.

In vivo *inhibition of PAR*. Activation of PARP in response to DNA damage results in ribosylation of various substrate proteins. To show inhibition of PARP activity *in vivo*, tumors from mice treated with ABT-888 were analyzed for levels of PAR by Western blot. B16F10 tumor-bearing mice were treated with either vehicle, temozolomide alone, or in combination with ABT-888 (Fig. 2C), similar to doses used in the efficacy study (Fig. 2A). A decrease in PAR proteins in tumors from animals treated with either ABT-888 alone or in combination with temozolomide was observed, indicating the ability of ABT-888 to inhibit PARP activity *in vivo*.

ABT-888 potentiates temozolomide in a syngeneic glioma model. ABT-888 also potentiates temozolomide in a 9L orthotopic rat glioma model. Maximum efficacy was seen at day 14 using magnetic resonance imaging (Fig. 3A and C). ABT-888 at 50 mg/kg/d in combination with temozolomide reduced tumor volume by 63%, which was 44% better than temozolomide alone ($P < 0.005$). Tumor growth inhibition with ABT-888 was dose dependent (Fig. 3A and B). The combination of 50 mg/kg/d dose of ABT-888 with temozolomide significantly prolonged animal survival versus temozolomide with a median survival of 19 and 22 days, respectively ($P < 0.0132$, log-rank test; Fig. 3B). ABT-888 as a single agent at

Downloaded from http://aacrjournals.org/clincancerres/article-pdf/13/9/2728/1974467/2728.pdf by guest on 28 February 2024

50 mg/kg/d was not efficacious in this model (data not shown). The combinations were well tolerated with maximum weight losses of only 9% for the combination compared with 8% for temozolomide.

To confirm central nervous system penetration, the pharmacokinetic profile of ABT-888 was evaluated in tumor-bearing rats with drug concentration measured in plasma as well as in brain and tumor tissues. After multiple doses of ABT-888 (50 mg/kg/d), the concentration of the compound 2 h after dosing (near C_{max}) was 1.36 ± 0.16 μg/mL, 0.72 ± 0.12 μg/g, and 3.00 ± 0.16 μg/g in plasma, brain, and tumor tissues, respectively. Coadministration of temozolomide did not alter the plasma pharmacokinetic profile of ABT-888 (data not shown).

ABT-888 potentiates platinum agents. The ability of ABT-888 to potentiate the efficacy of platinum-based agents was investigated in the MX-1 breast carcinoma xenograft model. This line was derived from a 29-year-old female with a poorly differentiated mammary carcinoma. Internal sequencing efforts at Abbott have determined that MX-1 has BRCA1 deletions. A novel *BRCA1* variant (*BRCA1 33636delGAAA*) was detected that would result in a frameshift mutation predicted to introduce a chain terminator and truncate the protein at residue 999. Two previously described nonsynonomous single-nucleotide polymorphisms were also detected in *BRCA2* (*BRCA2 16864A>C*, Asn^{289}His, and *BRCA2 221847A>G*, Asn^{991}Asp), both of which have been described in Chinese Breast Cancer families (33).

ABT-888 induced a pronounced potentiation of cisplatin activity (Fig. 4A). At day 68 when all mice were still present in each combination group, no significant differences were noted between the 5, 25, and 50 mg/kg/d combinations with cisplatin. However, at the end of the trial, ABT-888 at 5, 25, and 50 mg/kg/d in combination with cisplatin showed an increase in cures (8/9, 8/9, and 6/9 animals, respectively), whereas the cisplatin monotherapy had only 3/9 cures (no measurable tumors at end of the trial). Both the 5 and 25 mg/kg/d ABT-888 plus cisplatin were significantly different than cisplatin alone (P = 0.049, Fisher's exact test), whereas the 50 mg/kg/d ABT-888 was not significantly different from 5 and 25 mg/kg/d treatment combinations. The vehicle and ABT-888 monotherapy groups had no cures. This dose-response study showed that maximal potentiation was reached at 5 mg/kg/d ABT-888. Potentiation of platinum agents was confirmed in a second MX-1 study using carboplatin. Carboplatin is a second-generation platinum, less toxic anticancer drug and is currently the standard of care for treating lung, ovarian, and head and neck cancers. ABT-888 administered at 25 mg/kg/d via OMPs caused a pronounced potentiation of carboplatin at 10 and 15 mg/kg/d as reflected by tumor volumes (Fig. 4B). Compared with carboplatin treatment groups at day 38, the %T/C values were 34 (P = 0.011) and 18 (P < 0.0001) for the carboplatin 15 and 10 mg/kg/d combinations with ABT-888, respectively. The 10 mg/kg/d carboplatin/ABT-888 combination regressed tumor volumes from day 26, whereas carboplatin monotherapy had only a modest tumor inhibition.

Because ABT-888 showed a pronounced potentiation of carboplatin at 10 mg/kg/d, a separate study was undertaken to determine the dose-response relationship of ABT-888 at a fixed carboplatin dose. ABT-888 potentiated the activity of

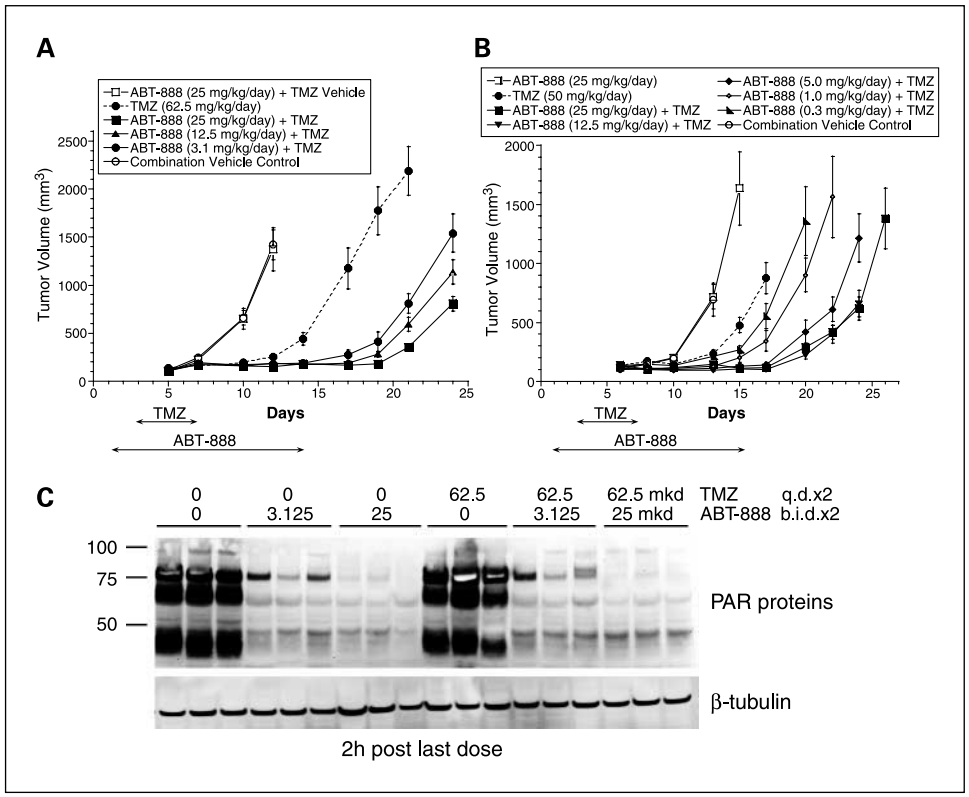

Fig. 2. Efficacy and biomarker response of ABT-888 in combination with temozolomide in B16F10 murine melanoma models. *A,* oral dose response of ABT-888. B16F10 cells were injected s.c. into C57BL/6 mice on day 0 and dosing was initiated on day 1. ABT-888 was administered p.o., b.i.d. on days 1 to 14. On days 3 to 7, temozolomide (TMZ; p.o., q.d.) was administered 2 h after ABT-888. Data consists of 8 to 10 mice per treatment group; bars, SE. *B,* ABT-888 continuous infusion dose response. B16F10 cells were injected on day 0. The 14-d OMPs were implanted s.c. on day 1 and temozolomide was administered p.o., q.d. on days 3 to 7. Data consists of 7 to 10 mice per treatment group; bars, SE. *C,* Western blot analysis showing significant inhibition in the level of poly(ADP-ribose) polymers in B16F10 flank tumors after treatment with ABT-888 alone or in combination with temozolomide. These results indicate inhibition of PARP activity in tumors after *in vivo* treatment and differential level of inhibition of PAR relative to dose of ABT-888. Mice were dosed with ABT-888 (25 and 3.125 mg/kg/d, p.o., b.i.d.×2) or temozolomide (62.5 mg/kg/d, p.o., q.d.×2) and in combination. Tumors were harvested 2 h after last dose.

Downloaded from http://aacrjournals.org/clincancerres/article-pdf/13/9/2728/1974467/2728.pdf by guest on 28 February 2024

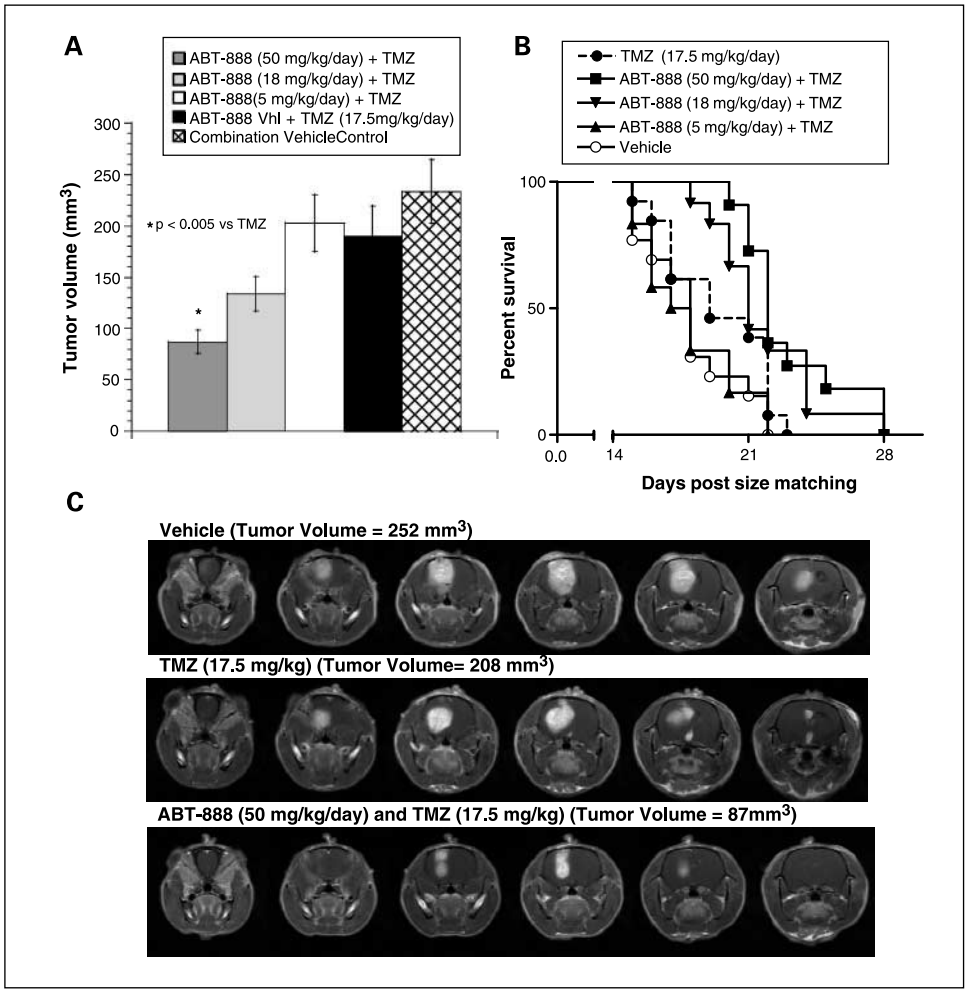

Fig. 3. *In vivo* efficacy of ABT-888 in combination with temozolomide in a syngeneic orthotopic 9L rat glioma model. *A,* glioma tumor volumes at day 14 using contrast-enhanced magnetic resonance imaging. Treatment of ABT-888 began on day 3 following tumor cell inoculation and continued for 13 d. Temozolomide was administered from day 4 to 8. Columns, mean of 11 to 12 rats per treatment group; bars, SE. ABT-888 as a single agent at 50 mg/kg/d was not efficacious in this model (data not shown). *B,* Kaplan-Meier analysis of orthotopic 9L rat glioma model (same experimental set of animals in *A*). Survival end point was based when animals showed signs of irreversible illness (e.g., impaired movement and greater than 20% weight loss). Median survival times for the vehicle, temozolomide, and 5, 18, and 50 ABT-888 mg/kg/d temozolomide combination groups were 18, 19, 17.5, 21, and 22 d, respectively. *C,* representative contrast-enhanced magnetic resonance images of orthotopic glioma (bright intensity areas) with the tumor volumes representative of the average for the treatment groups of vehicle, temozolomide alone, and ABT-888 and temozolomide. Row, transverse slices from a single rat taken on day 14.

10 mg/kg/d carboplatin (q4d×3) with %T/C values (versus carboplatin) at day 42 of 9 ($P < 0.0005$), 22 ($P = 0.0014$), and 42 ($P = 0.012$) for the 50, 25, and 12.5 mg/kg/d combinations of ABT-888 and carboplatin (data not shown). The 5 and 1 mg/kg/d doses of ABT-888 did not potentiate carboplatin.

ABT-888 potentiates cyclophosphamide. In the MX-1 model, ABT-888 administered at 25 mg/kg/d via OMPs not only potentiated cyclophosphamide at 12.5 mg/kg/d on days 20, 24, and 27 schedule (Fig. 4C) but also caused tumor regression, whereas the cyclophosphamide monotherapy only slightly delayed tumor growth. The %T/C values of this combination (versus cyclophosphamide) at day 38 was 35 ($P = 0.0011$). Cyclophosphamide was not effective at 5 mg/kg/d and ABT-888 did not potentiate the cytotoxic agent at this dose. In a separate confirmatory study, ABT-888 at 25 mg/kg/d enhanced the efficacy of cyclophosphamide (12.5 mg/kg/d, q4d×3) but potentiation was not shown at 12.5 mg/kg/d of ABT-888. The %T/C values of combinations (versus carboplatin) at day 42 were 53 ($P = 0.018$), 91 (not significant), and 100 (not significant) for the 25, 12.5, and 5 mg/kg/d doses of ABT-888 combinations, respectively (data not shown).

The ability of ABT-888 to potentiate the efficacy of cyclophosphamide was also evaluated in the DOHH-2 B-cell lymphoma flank xenograft model. DOHH-2 is a lymphoma line with the t(14;18) translocation that results in expression of high levels of Bcl-2 and is sensitive to cyclophosphamide (34). However, ABT-888 did not potentiate cyclophosphamide using an array of cytotoxic schedules (q.d.×1, q.d.×4, q4d×2, and q4d×3) and dosing schemes (data not shown), although cyclophosphamide showed single-agent activity. These data indicate that ABT-888 is not a potentiator of cyclophosphamide in the DOHH-2 model.

ABT-888 potentiates radiation. HCT-116 is a human colon cancer line that has been very well characterized for radiation sensitivity, including growth delay, cell cycle arrest, and apoptosis (35, 36). ABT-888 administered via OMPs at 25 mg/kg/d potentiated fractionated radiation (2 Gy/d × 10 days) with a median survival time of 36 days compared with 23 days ($P < 0.036$, log-rank test) from radiation alone (Fig. 5). Although ABT-888 did not enhance median survival (34 days) at 12.5 mg/kg/d ($P = 0.06$), this treatment group did have one cure (no palpable tumor) when the study was terminated on day 65. ABT-888 was also tested at 5 and 1 mg/kg/d in combination with radiation but these groups were not significantly different than radiation alone. Overall, ABT-888 showed a dose response in combination with radiation ($P = 0.0165$, log-rank trend).

Downloaded from http://aacrjournals.org/clincancerres/article-pdf/13/9/2728/1974467/2728.pdf by guest on 28 February 2024

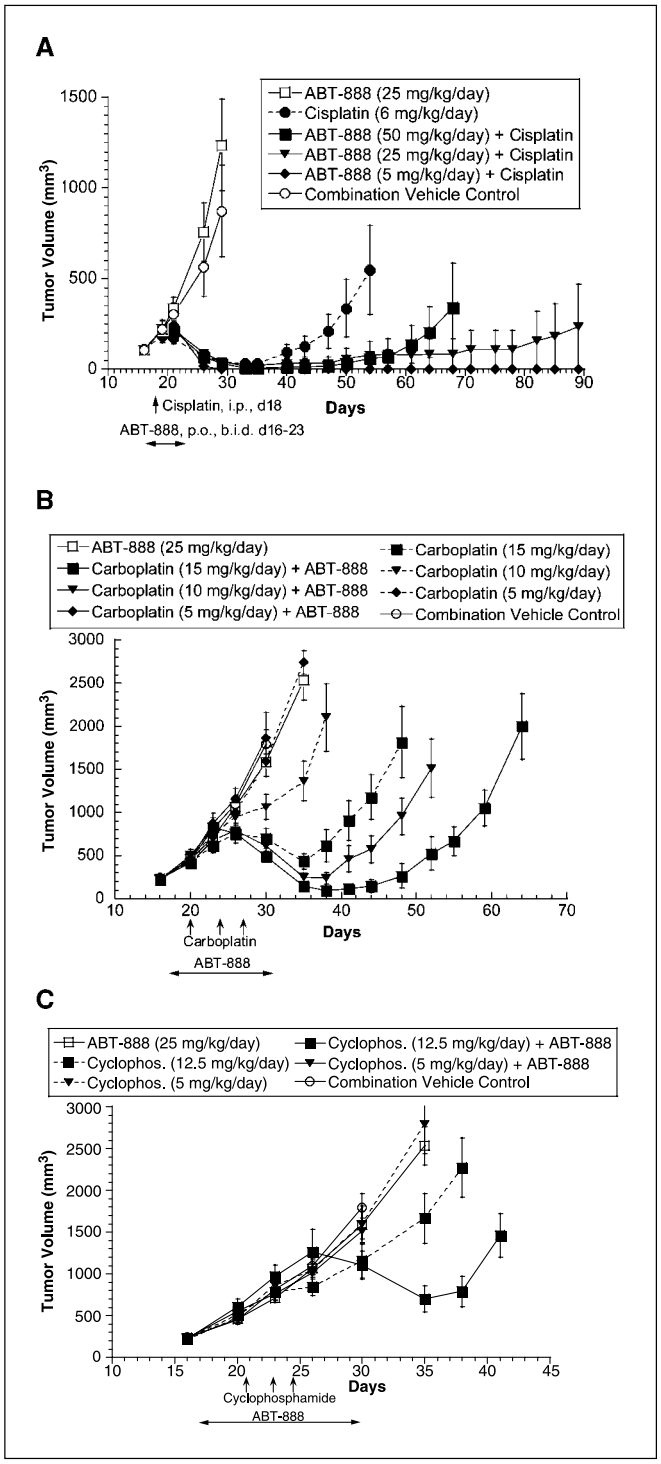

Fig. 4. *In vivo* efficacy of ABT-888 in combination with cisplatin, carboplatin, or cyclophosphamide in the MX-1 breast carcinoma xenograft model. *A,* tumors were size matched to 100 mm^3 on day 16 and PARP inhibitor therapy (p.o., b.i.d.×8) was initiated the same day. A single dose of cisplatin at 6.0 mg/kg/d was administered i.p. on day 18. Data consist of nine *nude* mice per treatment group; bars, SE. *B,* tumors were size matched to ~200 mm^3 on day 16. ABT-888 was administered at 25 mg/kg/d s.c., via 14-d OMPs starting on day 17. Carboplatin was administered i.p. on days 20, 24, and 27. Data consists of 8 to 10 *scid* mice per treatment group; bars, SE. *C,* tumors were size matched to ~200 mm^3 on day 16. ABT-888 was administered at 25, 12.5, and 5 mg/kg/d s.c., via 14-d OMPs starting day 17. Cyclophosphamide at 12.5 and 5 mg/kg/d was administered i.p., on days 20, 24, and 27. Data consist of 8 to 10 *scid* mice per treatment group; bars, SE. Respective control vehicles were used in all treatment groups.

Discussion

In this report, we describe ABT-888, a novel, orally bioavailable, PARP inhibitor that potentiates DNA-damaging agents. ABT-888 is a potent inhibitor of both PARP-1 and PARP-2 with K_is of 5.2 and 2.9 nmol/L, respectively. The compound is orally bioavailable in preclinical species and crosses the blood-brain barrier. ABT-888 induces a pronounced reduction in PAR proteins in tumor samples and this ability of ABT-888 to rapidly inhibit PARP *in vivo* confirms its favorable pharmacokinetic profile. The preclinical pharmacokinetic studies predicate that ABT-888 will have good human bioavailability suitable for either once or twice daily dosing that can be combined with cytotoxic agents. Several PARP inhibitors are under investigation in oncology clinical trials, including AG014699 (Pfizer) in combination with temozolomide in metastatic malignant melanoma (phase II); INO-1001 (Inotek/Genentech) in combination with temozolomide in malignant glioma (phase I); KU-59436, an oral compound from KuDOS/AstraZeneca as a single agent in cancer patients (phase I); and BS-201 (BiPar Sciences) as a monotherapy agent in phase I and ABT-888 in phase 0/Exploratory IND for dose refinements and pharmacokinetic relationships (24–26). An oral agent such as ABT-888, offers the cancer patient convenience when the overall therapy regimen likely includes parenterally administered combinations of varying schedules.

The favorable pharmacokinetic profile and potency of ABT-888 toward PARP enabled it to act as a broad-spectrum potentiator of DNA-damaging agents, including temozolomide, cisplatin, carboplatin, cyclophosphamide, and radiation. PARP inhibitors consistently potentiate temozolomide in preclinical studies, including experimental models of solid tumors (e.g., glioma, melanoma, colorectal, and breast cancer) and hematologic malignancies (lymphoid and nonlymphoid; refs. 25, 37, 38). Clinically, temozolomide is used to treat melanoma and in brain tumors. Metastatic melanoma is historically difficult to treat, with response rates for temozolomide and dacarbazine at just 13.5% and 12.1% and median overall survival of 7.7 and 6.4 months, respectively (39). Little change in overall survival has occurred for metastatic melanoma over the last 40 years. Temozolomide is used in combination with radiation to treat glioblastoma multiforme. This regimen provides brain tumor patients with a median overall survival of 14.6 months and a 2-year survival just over 25% (40). Clearly, these are both areas of high unmet medical needs and preclinical studies with ABT-888 in combination with temozolomide suggest the potential of improvement in therapy. ABT-888 strongly enhanced the activity of temozolomide in the B16F10 s.c. murine melanoma model regardless of the route of ABT-888 at doses as low as 3.1 mg/kg/d with maximal efficacy achieved at 25 mg/kg/d. In the treatment of brain tumors, the blood-brain barrier can significantly affect efficacy of agents (41). Brain and tumor tissue levels of 0.72 and 3.00 μg/g, respectively, confirm that ABT-888 can efficiently cross the blood-brain barrier. ABT-888 also potentiated temozolomide in the 9L orthotopic rat glioma model. Whereas temozolomide alone exhibited minimal efficacy, ABT-888 combined with temozolomide significantly slowed tumor progression (reflected in decreased tumor volume and prolonged survival) in a dose-related manner.

Downloaded from http://aacrjournals.org/clincancerres/article-pdf/13/9/2728/1974467/2728.pdf by guest on 28 February 2024

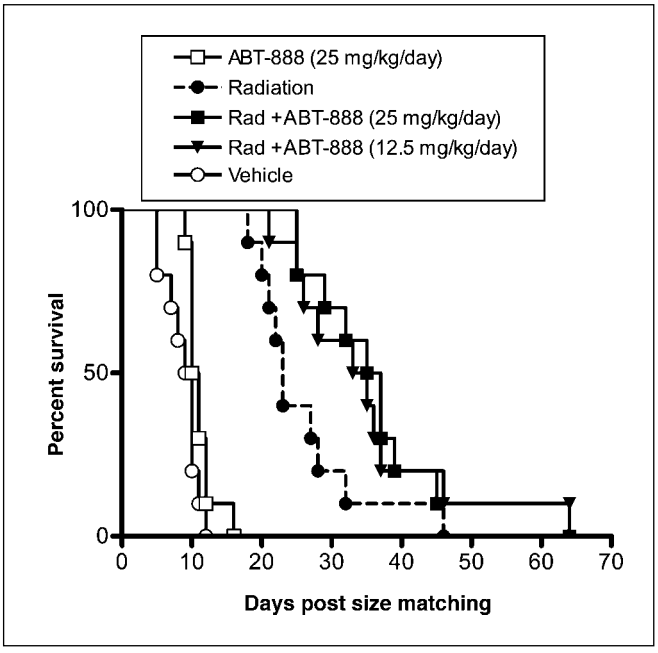

Fig. 5. Kaplan-Meier analysis of ABT-888 in combination with radiation in the HCT-116 colon carcinoma model. Cumulative survival (% of tumors for each group greater than 4× initial volume) is plotted versus time. Once a tumor volume of 100 to 200 mm^3 was reached, animals were randomly assigned to different treatment arms. ABT-888 was delivered via 14-d s.c. OMPs 3 d before radiation. Three days after pump implantation, groups of animals were chosen to receive once daily radiation (*Rad*) to the tumor xenograft site at 2 Gy per fraction for a total of 10 d. Median survival times for the vehicle, ABT-888 monotherapy, radiation, and 1, 5, 12.5, and 25 ABT-888 mg/kg/d radiation combination groups were 9.5, 10.5, 23, 25.5, 26.5, 34, and 36 d, respectively. In combination with radiation, ABT-888 showed a dose response ($P = 0.0165$, log-rank trend). ABT-888 at 5 and 1 mg/kg/d in combination with radiation was not plotted because these groups were not significantly different than radiation alone. Data consists of 10 mice per treatment group; bars, SE. Log-rank test of ABT-888 (25 mg/kg/d) combination versus radiation ($P = 0.036$); ABT-888 (12.5 mg/kg/d) combination versus radiation ($P = 0.06$). One animal had no measurable tumor at the end of the trial in the radiation and ABT-888 (12.5 mg/kg/d) combination group.

Ionizing radiation is the most widely used anticancer intervention after surgery inducing both single and dsDNA breaks. PARP inhibition results in radiosensitization through the impairment of both single- and double-stranded break repair pathways (42, 43), and PARP inhibitors have been shown to sensitize cancer cells to radiation, both *in vitro* and *in vivo* (17, 18, 25). In our study, ABT-888 potentiated fractionated radiation using the well-characterized radiosensitive HCT-116 colon model showing that an oral PARP inhibitor is an effective radiopotentiation agent. The strong potentiation of both temozolomide and radiation in preclinical settings is an incentive to consider using a PARP inhibitor with radiation in the glioma setting as well as for other tumor types.

Platinum agents are among the most widely used and effective anticancer drugs. These agents are used in the treatment for testicular, head and neck, ovarian, bladder, and lung cancers (44). Cytotoxic platinum agents (cisplatin, carboplatin, and oxaliplatin) form complex DNA adducts that damage DNA and lead to cell death. Enhanced DNA repair, through both the base excision repair and the nucleotide excision repair pathways, is a major mechanism by which tumor cells acquire resistance to these agents. Previous preclinical studies with cisplatin and PARP inhibitors showed only a mild *in vivo* potentiation of cisplatin in a NSCLC xenograft model (15) or were inactive *in vitro* (13). In contrast, ABT-888 at 5 mg/kg/d in combination with cisplatin caused sustained regressions resulting in 8/9 nonpalpable tumors versus 3/9 for cisplatin monotherapy. Our studies also show for the first time that a PARP inhibitor enhanced the activity of carboplatin. In two separate studies, ABT-888 potentiated carboplatin, causing tumor regression compared with only delayed tumor growth with carboplatin monotherapy (10 mg/kg/d). This prominent activity in a breast xenograft warrants further preclinical investigation in other tumor types given the broad clinical usage of platinum agents.

Cyclophosphamide is one of the most widely used alkylating agents and is effective in combination chemotherapy regimens for lymphoma, leukemia, breast cancer, small cell lung cancer, multiple myeloma, and sarcomas (45). Potentiation of this agent with a PARP inhibitor has not been reported previously *in vivo*. In our studies, ABT-888 potentiated cyclophosphamide, in the MX-1 breast xenograft model causing regressions of established tumors compared with tumor growth delay with cyclophosphamide monotherapy. However, the inability to potentiate another cyclophosphamide-sensitive model (DOHH-2 lymphoma) indicates that other factors, such as genetic mutations, may be important for PARP inhibitor activity.

One genetic factor that may be involved in PARP inhibitor profile responses is the BRCA status or more specifically homologous recombination competence (46). As described above, MX-1 xenograft model is sensitive to several cytotoxic agents, including carboplatin, cisplatin, and cyclophosphamide. Part of this sensitivity may be due to the dysfunction of DNA repair enzymes (47). BRCA-deficient lines are more sensitive to DNA-damaging agents and this sensitivity was translated to the clinic with BRCA1-associated ovarian carcinoma patients responding better to platinum-based therapies (48, 49). We have determined that MX-1 has BRCA1 deletions and contains a BRCA2 mutation but we do not know whether the BRCA2 mutation has any functional consequences. These genes are important for DNA double-strand break repairs by homologous recombination and these genetic alternations lead to a predisposition to breast and ovarian cancer. This is the first *in vivo* report of a PARP inhibitor in a human BRCA-deficient line in combination with cytotoxic agents (platinums and alkylating agents). The dramatic preclinical chemopotentiation of platinums and cyclophosphamide with a PARP inhibitor in the breast MX-1 model highlights their potential use in BCRA-deficient tumors, such as breast and ovarian as well as tumors with deficiency in proteins integral to homologous recombination (e.g., Rad51, ATM, and Fanconi anemia proteins). Due to our limited data set and in the absence of testing isogenic lines ±BRCA, it is still unclear whether BRCA or homologous recombination deficiencies are significant determinants of PARP inhibitor enhancements for platinum or cyclophosphamide antitumor activity; however, it may represent a useful clinical stratification strategy for a more robust efficacy signal. In addition, profiling of tumors for other DNA repair pathways and acquisition of their isogenic lines (e.g., *O*-6-methylguanine-DNA methyltransferase and mismatch repair) would further enhance clinical stratifications for temozolomide and other cytotoxics.

PARP inhibitors are also being evaluated as novel single-agent targeted cancer therapies. Recently, two reports suggested

Downloaded from http://aacrjournals.org/clincancerres/article-pdf/13/9/2728/1974467/2728.pdf by guest on 28 February 2024

that PARP inhibitors have activity against BRCA-deficient cells in the absence of any DNA-damaging agent (22, 23). Because not all BRCA-deficient cells are sensitive to the PARP inhibitors (50, 51), the prevalence of the single-agent cytotoxicity within the BRCA-deficient population is still not clear. In our studies, we observed no single-agent activity of ABT-888 in the MX-1 xenograft model as well as *in vitro* (data not shown). However, recently, it was shown that deficiencies in key homologous recombination genes is a major determinant in sensitivity to PARP single-agent inhibition and is not just confined to the BRCA1 or BRCA2 deficiencies (46). Other genetic defects or off-target axis activity of some PARP inhibitors may contribute to their single-agent antitumor activities. Regardless, because few BRCA-deficient xenograft models have been developed, the identification of MX-1 being BRCA deficient will be a very useful tool for understanding PARP inhibitor mechanisms for cancer monotherapy and combination therapy.

In summary, ABT-888 is an orally bioavailable PARP inhibitor that possesses an excellent efficacy and pharmacokinetic profile. The large unmet medical need and the potential for the broad use of this compound, in combination with numerous chemotherapeutic and radiotherapeutic regimens, renders ABT-888 an attractive agent for clinical development.

Acknowledgments

We thank Gail Bukofzer, Jason V. Brooks, Xueheng Cheng, Luciana Godzicki, Ruth Huang, Amanda Niquette, Lenette Paige, and Marion Refici (Abbott Laboratories) and Jennifer Marty (Cancer Therapy and Research Center, San Antonio, TX) for their excellent technical assistance.

Downloaded from http://aacrjournals.org/clincancerres/article-pdf/13/9/2728/1974467/2728.pdf by guest on 28 February 2024

References

1. Virág L, Szabó C. The therapeutic potential of poly(ADP-ribose) polymerase inhibitors. Pharmacol Rev 2002;54:375–429.
2. Shall S, de Murcia G. Poly(ADP-ribose) polymerase-1: what have we learned from the deficient mouse model? Mutat Res 2000;460:1–15.
3. Masutani M, Nozaki T, Nakamoto K, et al. The response of Parp knockout mice against DNA damaging agents. Mutat Res 2000;462:159–66.
4. Amé JC, Rolli V, Schreiber V, et al. PARP-2, a novel mammalian DNA damage-dependent poly(ADP-ribose) polymerase. J Biol Chem 1999;274:17860–8.
5. Menissier de Murcia J, Ricoul M, Tartier L, et al. Functional interaction between PARP-1 and PARP-2 in chromosome stability and embryonic development in mouse. EMBO J 2003;22:2255–63.
6. Tulin A, Chinenov Y, Spradling A. Regulation of chromatin structure and gene activity by poly(ADP-ribose) polymerases. Curr Top Dev Biol 2003;56:55–83.
7. Tomoda T, Kurashige T, Moriki T, et al. Enhanced expression of poly(ADP-ribose) synthetase gene in malignant lymphoma. Am J Hematol 1991;37:223–7.
8. Shiobara M, Miyazaki M, Ito H, et al. Enhanced polyadenosine diphosphate-ribosylation in cirrhotic liver and carcinoma tissues in patients with hepatocellular carcinoma. J Gastroenterol Hepatol 2001;16:338–44.
9. Hayaishi O, Ueda K. Poly(ADP-ribose) and ADP-ribosylation of proteins. Annu Rev Biochem 1977;46:95–116.
10. Fukushima M, Kuzuya K, Ota KIkai K. Poly(ADP-ribose) synthesis in human cervical cancer cell-diagnostic cytological usefulness. Cancer Lett 1981;14:227–36.
11. Schreiber V, Ame JC, Dolle P, et al. Poly(ADP-ribose) polymerase-2 (PARP-2) is required for efficient base excision DNA repair in association with PARP-1 and XRCC1. J Biol Chem 2002;277:23028–36.
12. Memisoglu A, Samson L. Base excision repair in yeast and mammals. Mutat Res 2000;451:39–51.
13. Curtin NJ, Wang LZ, Yiakouvaki A, et al. Novel poly(ADP-ribose) polymerase-1 inhibitor, AG14361, restores sensitivity to temozolomide in mismatch repair-deficient cells. Clin Cancer Res 2004;10:881–9.
14. Delaney CA, Wang LZ, Kyle S, et al. Potentiation of temozolomide and topotecan growth inhibition and cytotoxicity by novel poly(adenosine diphosphoribose) polymerase inhibitors in a panel of human tumor cell lines. Clin Cancer Res 2000;6:2860–7.
15. Miknyoczki SJ, Jones-Bolin S, Pritchard S, et al. Chemopotentiation of temozolomide, irinotecan, and cisplatin activity by CEP-6800, a poly(ADP-ribose) polymerase inhibitor. Mol Cancer Ther 2003;2:371–82.
16. Tentori L, Leonetti C, Scarsella M, et al. Systemic administration of GPI 15427, a novel poly(ADP-ribose) polymerase-1 inhibitor, increases the antitumor activity of temozolomide against intracranial melanoma, glioma, lymphoma. Clin Cancer Res 2003;9:5370–9.
17. Calabrese CR, Almassy R, Barton S, et al. Anticancer chemosensitization and radiosensitization by the novel poly (ADP-ribose) polymerase-1 inhibitor AG14361. J Natl Cancer Inst 2004;96:56–67.
18. Veuger SJ, Curtin NJ, Richardson CJ, Smith GC, MDurkacz BW. Radiosensitization and DNA repair inhibition by the combined use of novel inhibitors of DNA-dependent protein kinase and poly(ADP-ribose) polymerase-1. Cancer Res 2003;63:6008–15.
19. Lindahl T, Wood RD. Quality control by DNA repair: frontiers in cell biology: quality control. Science 1999;286:1897–905.
20. Masutani M, Nozaki T, Nishiyama E, et al. Function of poly(ADP-ribose) polymerase in response to DNA damage: gene-disruption study in mice. Mol Cell Biochem 1999;193:149–52.
21. de Murcia JM, Niedergang C, Trucco C, et al. Requirement of poly(ADP-ribose) polymerase in recovery from DNA damage in mice and in cells. Proc Natl Acad Sci U S A 1997;94:7303–7.
22. Farmer H, McCabe N, Lord CJ, et al. Targeting the DNA repair defect in BRCA mutant cells as a therapeutic strategy. Nature 2005;434:917–21.
23. Bryant HE, Schultz N, Thomas HD, et al. Specific killing of BRCA2-deficient tumours with inhibitors of poly (ADP-ribose) polymerase. Nature 2005;434:913–7.
24. Sheridan C. Genentech raises stakes on PARP inhibitors. Nat Biotechnol 2006;24:1179–80.
25. Plummer ER. Inhibition of polyADP-ribose polymerase in cancer. Curr Opin Pharmacol 2006;6:364–8.
26. Kinders RJ, Palma J, Liu X, et al. Development of a quantitative enzyme immunoassay for measurement of PAR as a pharmacodynamic biomarker of PARP activity. In: The First AACR International Conference on Molecular Diagnostics in Cancer Therapeutic Development: Maximizing Opportunities for Individualized Treatment; 2006; Chicago, IL.
27. Zhu GD, Gong J, Gandhi V, Penning TD, Giranda VL. 1H-Benzimidazole-4-carboxamides substituted with a quaternary carbon at the 2-position are potent parp inhibitors. United States patent application 2006/0229289. 2006.
28. Marcotte PA, Richardson PL, Guo J, et al. Fluorescence assay of SIRT protein deacetylases using an acetylated peptide substrate and a secondary trypsin reaction. Anal Biochem 2004;332:90–9.
29. Yee KWL, Hagey A, Verstovsek S, et al. Phase 1 study of ABT-751, a novel microtubule inhibitor, in patients with refractory hematologic malignancies. Clin Cancer Res 2005;11:6615–24.
30. Honore P, Donnelly-Roberts D, Namovic MT, et al. A-740003 [*N*-(1-{[(cyanoimino)(5-quinolinylamino) methyl]amino}-2,2-dimethylpropyl)-2-(3,4-dimethoxyphenyl)acetamide], a novel and selective P2X7 receptor antagonist, dose-dependently reduces neuropathic pain in the rat. J Pharmacol Exp Ther 2006;319:1376–85.
31. Houghton PJ, Stewart CF, Thompson J, et al. Extending principles learned in model systems to clinical trials design. Oncology 1998;12:84–93.
32. Lapidus RG, Tentori L, Graziani G, et al. Oral administration of PARP inhibitor GPI 18180 increases the anti-tumor activity of temozolamide against intracranial melanoma in mice. J Clin Oncol 2005;23:3136.
33. Zhou YZ, Sun Q, Lin SQ, et al. Germline mutations in the BRCA1 and BRCA2 genes from breast cancer families in China Han people. Zhonghua Yi Xue Za Zhi 2004;84:294–8.
34. Wong FMP, Bally M, B.Klasa R. Low dose antisense oligonucleotides to bcl-2 with cyclophosphamide cures SCID/Rag-2 mice with a human B cell lymphoma. In: 90th Annual Meeting of the American Association for Cancer Research; 1999 April 10–14; Philadelphia, Pennsylvania, USA. American Association for Cancer Research. Proceedings of the American Association for Cancer Research Annual Meeting. 1999.
35. Waldman T, Kinzler KW, Vogelstein B. p21 is necessary for the p53-mediated G_1 arrest in human cancer cells. Cancer Res 1995;55:5187–90.
36. Bunz F, Dutrlaux A, Lengauer C, et al. Requirement for p53 and p21 to sustain G_2 arrest after DNA damage. Science 1998;282:1497–501.
37. Tentori L, Graziani G. Chemopotentiation by PARP inhibitors in cancer therapy. Pharmacol Res 2005;52:25–33.
38. Curtin NJ. PARP inhibitors for cancer therapy. Expert Rev Mol Med 2005;7:1–20.
39. Middleton MR, Grob JJ, Aaronson N, et al. Randomized phase III study of temozolomide versus dacarbazine in the treatment of patients with advanced metastatic malignant melanoma. J Clin Oncol 2000;18:158–66.
40. Stupp R, Mason WP, van den Bent MJ, et al. Radiotherapy plus concomitant and adjuvant temozolomide for glioblastoma. N Engl J Med 2005;352:987–96.
41. Newlands ES, Stevens MF, Wedge SR, Wheelhouse RT, Brock C. Temozolomide: a review of its discovery, chemical properties, pre-clinical development, and clinical trials. Cancer Treat Rev 1997;23:35–61.
42. Benjamin RC, Gill DM. Poly ADP ribose synthesis *in vitro* programmed by damaged DNA: a comparison of DNA molecules containing different types of strand breaks. J Biol Chem 1980;255:10502–8.
43. Boulton S, Kyle S, Durkacz BW. Interactive effects of inhibitors of poly(ADP-ribose) polymerase and DNA-dependent protein kinase on cellular responses to DNA damage. Carcinogenesis 1999;20:199–203.
44. O'Dwyer PJ, Johnson SW, Hamilton TC.

Pharmacology of cancer chemotherapy: cisplatin and its analogues. In: DeVita VT, Jr., Hellman S, Rosenberg SA, editors. Cancer: Principles and practice of oncology. Philadelphia (PA): Lippincott-Raven Publishers; 1997. p. 418–32.

45. Teicher BA. Antitumor alkylating agents. In: DeVita VT, Jr., Hellman S, Rosenberg SA, editors. Cancer: principles and practice of oncology. Philadelphia (PA): Lippincott-Raven Publishers; 1997. p. 405–18.

46. McCabe N, Turner NC, Lord CJ, et al. Deficiency in the repair of DNA damage by homologous recombination and sensitivity to polyADP-ribose polymerase inhibition. Cancer Res 2006;66:8109–15.

47. Caldecott KW, Chalmers A. An Achilles' heel for breast cancer? Nat Struct Mol Biol 2005;12: 387–8.

48. Xing D, Orsulic S. A mouse model for the molecular characterization of BRCA1-associated ovarian carcinoma. Cancer Res 2006;66:8949–53.

49. Cass I, Baldwin RL, Varkey T, et al. Improved survival in women with BRCA-associated ovarian carcinoma. Cancer 2003;97:2187–95.

50. De Soto JA. Deng C-X. PARP-1 inhibitors: are they the long-sought genetically specific drugs for BRCA1/2-associated breast cancers? Int J Med Sci 2006;3:117–23.

51. De Soto JA, Wang X, Tominaga Y, et al. The inhibition and treatment of breast cancer with poly (ADP-ribose) polymerase (PARP-1) inhibitors. Int J Biol Sci 2006;2:179–85.

Downloaded from http://aacrjournals.org/clincancerres/article-pdf/13/9/2728/1974467/2728.pdf by guest on 28 February 2024